Available online at www.sciencedirect.com
SCIENCE DIRECT®
Journal of the European Ceramic Society 24 (2004) 3499–3508
www.elsevier.com/locate/jeurceramsoc

A novel process for the synthesis of cordierite ($Mg_2Al_4Si_5O_{18}$) powders from rice husk ash and other sources of silica and their comparative study

Milan Kanti Naskar*, Minati Chatterjee

Sol-Gel Division, Central Glass and Ceramic Research Institute, 196 Raja S.C. Mullick Road, Jadavpur, Kolkata 700 032, India

Received 6 June 2003; received in revised form 6 November 2003; accepted 21 November 2003

Available online 14 April 2004

Abstract

Cordierite ($Mg_2Al_4Si_5O_{18}$) powders were synthesised by utilising agro-based 'waste' material-rice husk ash and two other sources of silica, i.e. tetraethylorthosilicate (TEOS) and fumed silica, for a comparative study following sol–gel technique. The gel and calcined powders obtained from different silica sources were characterised by thermogravimetry analysis (TGA), differential thermal analysis (DTA), X-ray diffraction (XRD) study, Fourier transformed infrared (FTIR) spectroscopy, ^{27}Al and ^{29}Si solid state MAS NMR spectroscopy, scanning electron microscopy (SEM) and particle size analysis. For rice husk ash as the source material, DTA and XRD results confirmed that α-cordierite was formed at 1365 °C through the intermediate phases of cristobalite and $MgAl_2O_4$ spinel while in case of TEOS and fumed silica sources, α-cordierite formed at 1320 and 1360 °C respectively through the intermediate phases of μ-cordierite and magnesium aluminate ($MgAl_2O_4$) spinel for the former and via the $MgAl_2O_4$ spinel for the latter. FTIR studies showed the vibration bands of SiO_4 tetrahedra, AlO_6 octahedra and AlO_4 tetrahedra for different sources of silica calcined at different temperatures. The ^{27}Al solid state NMR confirmed the highly abundance of AlO_6 octahedra while ^{29}Si solid state NMR revealed the Q^4 state for SiO_4 tetrahedra for the sample obtained from rice husk ash after calcination at 800 °C. The SEM showed the irregular morphology of the calcined powders (1400 °C) for all the samples and comparatively wide size distribution of the particles was found for the sample obtained from rice husk ash.

Keywords: Sol–gel processes; X-ray methods; Structural applications; Cordierite; Rice husks

1. Introduction

Cordierite ($Mg_2Al_4Si_5O_{18}$) ceramics because of its low thermal expansion co-efficient and high refractoriness[1,2] is a promising candidate as a structural material and find applications as a carrier of catalyst for exhaust gas control in automobiles, heat exchangers for gas turbine engines, industrial furnaces, packing materials in electronic packing, refractory coatings on metals, etc. It is also used as an integrated circuit substrate because of low dielectric constant.[3,4]

The conventional methods of cordierite powder synthesis include sintering of oxide powders through solid state reactions or crystallising the glasses.[3–5] However, because of some inherent difficulties of the above mentioned methods,[3,6] much of the recent work on cordierite powder synthesis uses different varieties of the sol–gel and related techniques.[7,8] Douy[8] exploited an elaborate organic gel method (with or without citric acid) for obtaining cordierite powders. In addition to that, the combustion technique[9] for the synthesis of cordierite is worth mentioning. Each of these methods has its own respective advantages and disadvantages. Further, the choice of the starting materials, e.g. soluble metal salts, metal alkoxides, colloidal suspensions, their availability, the steps involved during sol and gel formation along with the processing time are some of the important points to be taken into consideration during the synthesis of the materials.

Rice husk is an abundantly available agricultural waste material and the burnt rice husk causes environmental pollution.[10] In the present investigation, an effort has been made to find the value addition to rice husk ash in synthesising advanced ceramic material like cordierite. Keeping this view in mind, in respect of environmental friendly and cost-effectiveness, the cordierite powders were synthesised

* Corresponding author.
E-mail address: milan312@hotmail.com (M.K. Naskar).

0955-2219/$ – see front matter © 2004 Elsevier Ltd. All rights reserved.
doi:10.1016/j.jeurceramsoc.2003.11.029

starting from rice husk ash and other water-based precursor materials following a simple step wet-chemical process. For a comparative study, the same powders were also synthesised with other sources of silica, i.e. tetraethylorthosilicate (TEOS) and fumed silica following the same experimental procedure as done in case of rice husk ash as source material. The powders obtained from rice husk ash and other sources of silica were characterised by their thermal analysis, crystallisation behaviour study, FTIR spectroscopy, ^{27}Al and ^{29}Si solid state NMR spectroscopy, SEM and particle size analysis.

2. Experimental

2.1. Preparation of sols, gels and oxide powders

Fig. 1 presents the flow diagram for the synthesis of cordierite ($Mg_2Al_4Si_5O_{18}$) powders from sol–gel method using rice husk ash and other sources of silica, i.e. TEOS and fumed silica. For the preparation of sols with cordierite composition, i.e. $2MgO{\cdot}2Al_2O_3{\cdot}5SiO_2$, two steps were followed: (i) preparation of bi-component sol of magnesia–alumina with their stoichiometric compositions; and (ii) preparation of tri-component sol of magnesia–alumina–silica with their stoichiometric compositions by the addition of different silica sources to the bicomponent sol prepared as above (i).

In the first step, the precursor materials for the preparation of magnesia–alumina (2:2 mole ratio) sol were hydrated aluminium nitrate, $Al(NO_3)_3{\cdot}9.15H_2O$ (A.R., Merck India, purity >99%) and hydrated magnesium nitrate, $Mg(NO_3)_2{\cdot}6.12H_2O$ (A.R., Merck India, purity >99%). Calculated quantities of $Mg(NO_3)_2{\cdot}6.12H_2O$ and $Al(NO_3)_3{\cdot}9.15H_2O$ were dissolved in measured volume of deionised water (conductivity of water: 1.4×10^{-5} S) to make a solution of 1 M with respect to Al^{3+}. The pH of the bi-component solution was then adjusted at room temperature (RT), to about 3 by the addition of concentrated ammonia solution (25 wt.%, G.R., Merck, India) under stirring. The resulting sol was then heated to $80 \pm 1\,^{\circ}C$ under controlled condition, i.e. by dropwise addition of concentrated ammonia solution under vigorous stirring in a covered container.[11,12] The viscosity of the sol thus obtained increased with increasing time of heating. The heating was continued until the final viscosity of the clear, transparent, composite sols was determined to be 25 ± 1 mPa s. The pH of the sol at this stage was

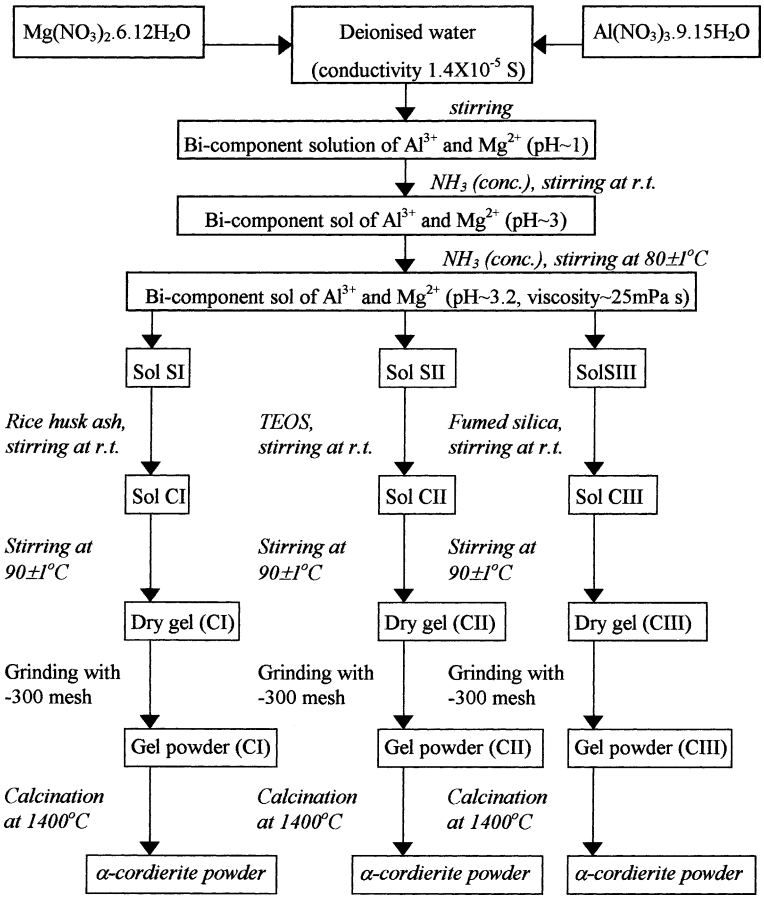

Fig. 1. A flow diagram for the synthesis of cordierite powders from different silica sources.

found to be 3.2. The pH of the sols was measured with a Jencon pH meter (Model 3030) while the viscosity values were recorded using a Brookfield Viscometer (Model LVTDV-II). The bi-component sol of magnesia–alumina thus obtained was divided into three parts namely SI, SII and SIII.

In the second step, calculated quantities of rice husk ash (laboratory made, crystalline form: crystobalite, composition (wt.%): SiO_2 (90.23%), TiO_2 (0.13%), Al_2O_3 (1.07%), Fe_2O_3 (0.27%), CaO (0.39%), MgO (0.18%), K_2O (1.36%), P_2O_5 (2.38%), L.O.I. (3.99%)) and other sources of silica, i.e. TEOS (Fluka Chemica, Purum grade) and fumed silica (Cab-O-Sil, Cabot Corporation, 95.84 wt.% SiO_2) were added under stirring at RT to the bi-component sols of SI, SII and SIII, respectively. The addition of TEOS to the bicomponent sol at pH 3.2 formed an immiscible sol at the initial stage, but with the progress of hydrolysis reaction of TEOS at the above pH, alcohol was produced as the by-product which was sufficient to homogenise the initial immiscible phase.[13] The three different tricomponent sols of magnesia–alumina–silica, containing rice husk ash, TEOS and fumed silica as the silica sources were prepared and they were designated as CI, CII and CIII respectively (Fig. 1).

The three different sols, CI, CII and CIII containing magnesia, alumina and silica in their stoichiometric compositions were continuously heated at $90 \pm 1\,^{\circ}C$ under stirring to obtain the corresponding gel powder of CI, CII and CIII. The agglomerated gels were ground to make −300 mesh powders. The gel powders thus obtained were subjected to calcination from 400 to 1400 °C each, with a heating rate of 3.3 °C/min and with a dwell time of 1 h under a programmable furnace in static air condition.

2.2. Characterisation of gels and oxide powders

The gel powders were characterised by differential thermal analysis (DTA) and thermogravimetry (TG) (Netzsch STA 409c) from 30 to 1400 °C in Ar atmosphere at the heating rate of 10 °C/min. Crystalline phases of the calcined powders developed at different temperatures were examined by X-ray diffraction (XRD, Philips PW-1730) with Ni-filtered Cu Kα radiation. The IR vibrational spectroscopy of different gel and calcined samples (CI, CII and CIII) was performed with Fourier transform infrared (FTIR) study (Nicolet 5 PC) in the wavenumber range 4000–400 cm^{-1} using 4.0 cm^{-1} resolution. The ^{27}Al and ^{29}Si MAS NMR of the samples CI, CII and CIII calcined at 800 °C/1 h dwell time were obtained with a Bruker DSX-300 solid state FT-NMR spectrometer at 78.2 MHz (^{27}Al) and 59.6 MHz (^{29}Si) with the spinning frequencies of 5 kHz and 1000 number of scans for ^{27}Al and 7 kHz and 2000 number of scans for ^{29}Si at the magic angle of 54.7°. The chemical shifts were given in ppm with respect to the external standard of 1 M $Al(NO_3)_3$ for ^{27}Al and tetramethyl silane (TMS) for ^{29}Si.

3. Results and discussion

3.1. Thermal analysis by DTA and TG

DTA curves for the sample CI obtained from rice husk ash source shows two broad endothermic peaks at 145 and 329 °C (Fig. 2a) while for the sample CII (obtained from TEOS) and CIII (obtained from fumed silica), the corresponding endothermic peaks were at 181 and 299 °C for the former (Fig. 2b) and at 156 and 302 °C for the latter (Fig. 2c). From the TG curves of the samples CI, CII and CIII, it is clear that a total weight loss of about 21–22% occurred in the temperature region 30–250 °C (Fig. 2a–c). However, in the temperature region 250–500 °C, the weight loss for the sample CI was 15.10% (Fig. 2a) and those for the samples CII (Fig. 2b) and CIII (Fig. 2c) were 23.72 and 13.79%, respectively. The peak temperatures obtained from DTA curves and percent of weight loss obtained from TG curves for all the samples CI, CII and CIII are also shown in a tabular form (Table 1 for DTA and Table 2 for TG).

The first endothermic peak temperatures, i.e. 145, 181 and 156° C for the samples, CI, CII and CIII were attributed to the removal of absorbed water and other volatiles present in the gel samples.[7] It is to be noted here that for the gel sample CI obtained from rice husk ash, the endothermic peak

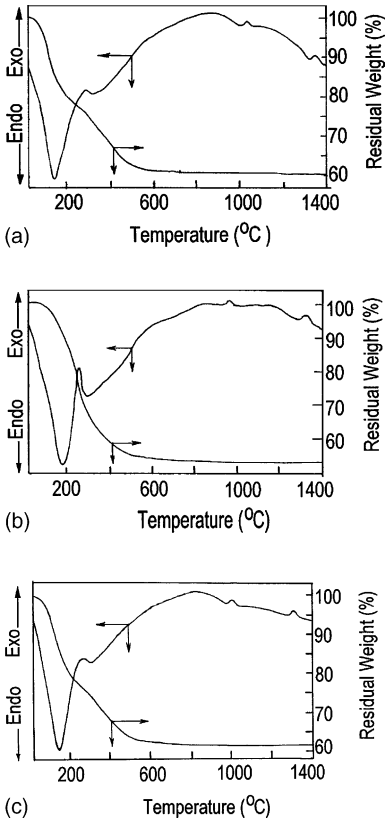

Fig. 2. (a) DTA and TG curves of the powder sample CI obtained from rice husk ash. (b) DTA and TG curves of the powder sample CII obtained from TEOS. (c) DTA and TG curves of the powder sample CIII obtained from fumed silica.

Table 1
DTA results of the precursor cordierite gel powder

Sample designation	Peak temperature (°C)	
	Endothermic	Exothermic
CI	145, 329	298, 1039, 1365
CII	181, 299	962, 1319
CIII	156, 302	1008, 1362

temperature was lower compared to that of the gel samples CII and CIII; there occurred rather a more easy escape of absorbed water molecules from CI compared to CII and CIII. The second broad endothermic peaks at 329, 299 and 302 °C for the samples CI, CII and CIII, respectively (Fig. 2a–c) are due to the removal of structural hydroxyl groups[7,14] and the decomposition of nitrate ions.[7,15,16] For TG results, in the temperature region 250–500 °C, it is clear that there occurred a minimum amount of weight losses of 15.10 and 13.79% for CI and CIII, respectively, compared to the sample CII (23.72% weight loss). From the TG results in the temperature region 250–500 °C it can be pointed out that a good number of structural hydroxyl groups and carbon moities were removed accompanying with a maximum amount of weight loss from the sample CII compared to CI and CIII.

The exothermic peaks observed in the temperature region 960–1365 °C for the gel samples CI, CII and CIII indicated the crystallisation of different phases, as it was revealed from the TG curve, in the temperature region 750–1400 °C (Fig. 1a–c), there occurred practically no weight loss. The first exothermic peak identified at 298 °C for the sample CI (obtained from rice husk ash) was due to the crystallisation of cristobalite. The other two exothermic peaks appeared at 1039 and 1365 °C for the sample CI corroborated to the crystallisation of $MgAl_2O_4$ spinel and α-cordierite, respectively. For the sample CII, the exothermic peak at 962 °C was due to the crystallisation of $MgAl_2O_4$ spinel and μ-cordierite[17] and another exothermic peak at 1319 °C corresponded to the crystallisation of α-cordierite. For the sample CIII, the exothermic peaks observed at 1008 and 1362 °C indicated the crystallisation of $MgAl_2O_4$ spinel and α-cordierite, respectively.

It is to be noted that gel samples CI, CII and CIII were heated separately in Ar atmosphere to the corresponding exothermic peak temperatures obtained from DTA results with the same heating rate (10 °C/min) and quenching to room temperature as done in DTA analysis. The heated samples were analysed by XRD which confirmed the crystallisation of the respective phases as observed from the exothermic peaks of DTA curves.

3.2. Crystallisation behaviour of the gel powders by XRD

To study the crystallisation behaviour of the phases appeared at different temperatures, XRD patterns of the gel powders corresponding to the samples CI, CII and CIII, heat-treated at 400, 600, 800, 1000, 1200, 1300 and 1400 °C each with a dwell time of 1 h, were recorded. The crystalline phases developed at different temperatures for the samples CI, CII and CIII are shown in Fig. 3a(I, II), b(I, II) and c(I, II) respectively. For the sample CI obtained from rice husk ash, Fig. 3a(I) reveals that at 400 and 600 °C, only the cristobalite phase was identified; however, it was also observed by XRD that crystallisation of cristobalite occurred at 300 °C with the heating rate (10 °C/min) as done in DTA analysis. With increase in temperature up to 800 °C a trace amount of $MgAl_2O_4$ spinel phase was found in presence of cristobalite (Fig. 3a(I)), and the former phase increased with increasing temperature up to 1200 °C (Fig. 3a(II)). At 1300 °C, with the disappearance of cristobalite phase, α-cordierite phase was becoming the major phase in presence of minor amount of $MgAl_2O_4$ spinel phase (Fig. 3a(II)). At 1400 °C, almost complete transformation of α-cordierite phase took place along with a trace amount of $MgAl_2O_4$ spinel phase (Fig. 3a(II)).

For the sample CII obtained from TEOS, Fig. 3b(I) reveals that up to 800 °C it remained amorphous. However, crystallisation of μ-cordierite and $MgAl_2O_4$ spinel phase appeared at 1000 °C and it remained up to 1200 °C (Fig. 3b(II)). With increase in temperature up to 1300 °C, a substantial increase of α-cordierite took place containing a small amount of $MgAl_2O_4$ spinel and μ-cordierite (Fig. 3b(II)). A complete transformation of α-cordierite occurred at 1400 °C (Fig. 3b(II)).

For the sample CIII obtained from fumed silica, Fig. 3c(I) shows that at 400–800 °C, some small humps corresponded to amorphous silica and $MgAl_2O_4$ spinel appeared. A sharp crystallisation of $MgAl_2O_4$ spinel occurred at 1000 °C (Fig. 3c(II)) and it retained up to 1200 °C where silica remained still amorphous. With increase in temperature up to 1300 °C, α-cordierite substantiated containing a small amount $MgAl_2O_4$ spinel phase (Fig. 3c(II)). At 1400 °C, only α-cordierite phase was observed (Fig. 3c(II)).

Table 2
TG results of the precursor cordierite gel powder

Sample designation	Weight loss (%) at different temperature (°C) regions				Total wt. loss (%)
	30–250	250–500	500–750	750–1400	
CI	22.02	15.10	2.18	0.44	39.74
CII	21.10	23.72	1.92	0.17	46.91
CIII	22.36	13.79	2.01	0.15	38.21

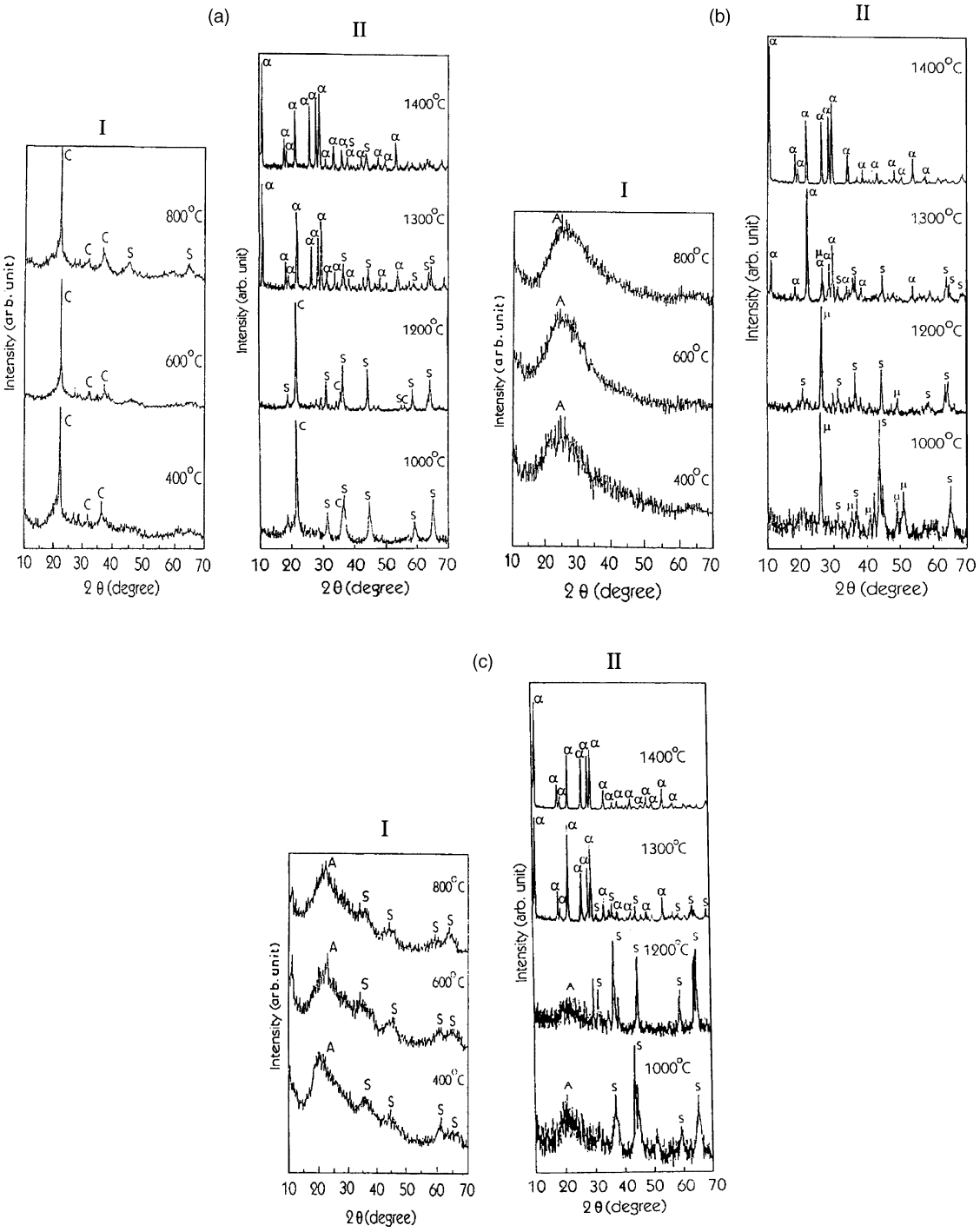

Fig. 3. (a) XRD patterns of the powder sample CI obtained from rice husk ash, (I) calcined at 400–800 °C and (II) calcined at 1000–1400 °C; C: cristobalite; S: $MgAl_2O_4$ spinel; α: α-cordierite. (b) XRD patterns of the powder sample CII obtained from TEOS, (I) calcined at 400–800 °C and (II) calcined at 1000–1400 °C; A: amorphous silica; μ: μ-cordierite; S: $MgAl_2O_4$ spinel; α: α-cordierite; (c) XRD patterns of the powder sample CIII obtained from fumed silica, (I) calcined at 400–800 °C and (II) calcined at 1000–1400 °C; A: amorphous silica; S: $MgAl_2O_4$ spinel; α: α-cordierite.

From the XRD results it is noteworthy that for the sample CI, crystallisation of silica as cristobalite occurred at lower temperature (300 °C) following the formation of $MgAl_2O_4$ at 1000 °C which interacted with the former to generate α-cordierite at 1300 °C. However, for the sample CII, α-cordierite phase generated through the intermediate phases of μ-cordierite and $MgAl_2O_4$ spinel. In case of CIII, the only intermediate phase of $MgAl_2O_4$ took part in reaction with amorphous silica at about 1000 °C towards the formation of α-cordierite at higher temperature (1300 °C). The peaks of cristobalite, $MgAl_2O_4$ spinel, μ-cordierite and α-cordierite observed in the XRD patterns of different

samples, matched well with the corresponding peaks reported in the JCPDS International Centre for Diffraction Data, File Nos. 39-1425, 21-1152, 14-249 and 13-293 respectively.

3.3. FTIR spectroscopy

To investigate the structural changes occurred towards the formation of cordierite through the different phase transitions of the powders CI, CII and CIII, each calcined at 800, 1000, 1200, 1300 and 1400 °C, FTIR studies were performed in the wavenumber range 4000–400 cm^{-1}; however, the spectra in the wavenumber region 1300–400 cm^{-1} are presented for the samples CI, CII and CIII in Fig. 4a–c, respectively. For the calcined samples at 800–1200 °C, a characteristic shoulder in the region 1100–1000 cm^{-1} appeared in all the samples (CI, CII and CIII) which corresponded to the presence of Si–O–Si asymmetric stretching vibration while that observed at about 950–930 cm^{-1} for the samples CI (Fig. 4a) and CIII (Fig. 4c) calcined at 1300–1400 °C and for the sample CII calcined at 1000–1400 °C (Fig. 4b) indicated the character of symmetric stretching of AlO_4 tetrahedra.[4] The band at around 770 cm^{-1} for all the samples, CI, CII and CIII calcined at 1300–1400 °C was due to the symmetric stretching mode of the Si–O–Si bond.[4,18] It was clear that the strong bands at around 650 and 600 cm^{-1} for CI, CII and CIII were due to condensed AlO_6 octahedra[19–22] and that appeared around 580 and 470 cm^{-1} were assigned to the Al–O stretching vibration in isolated AlO_6 octahedra.[5]

For the sample CI and CIII calcined at 800–1200 °C, the characteristic bands of $MgAl_2O_4$ spinel were observed at around 800 and 700 cm^{-1}. For the sample CII calcined at 1000–1300 °C, the absorption bands at around 1085, 935, 700, 460 cm^{-1} were assigned to the formation of μ-cordierite (Fig. 4b) while the bands at around 790, 700 and 560 cm^{-1} at the same temperature region were the characteristics of $MgAl_2O_4$ spinel.[7,22] The characteristic peaks of α-cordierite[3] were found at around 1185, 1140, 950, 770, 680, 615, 580, 480 and 430 cm^{-1} for the samples CI, CII and CIII calcined at 1300–1400 °C (Fig. 4a–c).

3.4. ^{27}Al and ^{29}Si MAS NMR spectroscopy

Fig. 5a presents ^{27}Al MAS NMR of CI, CII and CIII calcined at 800 °C/1 h dwell each. The temperature at 800 °C was chosen to investigate the relative abundance of $[AlO_4]$ tetrahedra and $[AlO_6]$ octahedra and the ordering of $[SiO_4]$ tetrahedra in the structure before the formation of cordierite at higher temperature. The peak in the region 55–77 ppm was attributed to the tetrahedrally co-ordinated Al sites, Al(IV) whereas the peak around −2 to 10 ppm was assigned to octahedrally co-ordinated Al sites, Al(VI).[23–26] The small shift in the spectra (Fig. 5a) resulted due to the nature of the environment in which Al(IV) and/or Al(VI) interacted with $[SiO_4]$ tetrahedra. It is to be noted that the relative

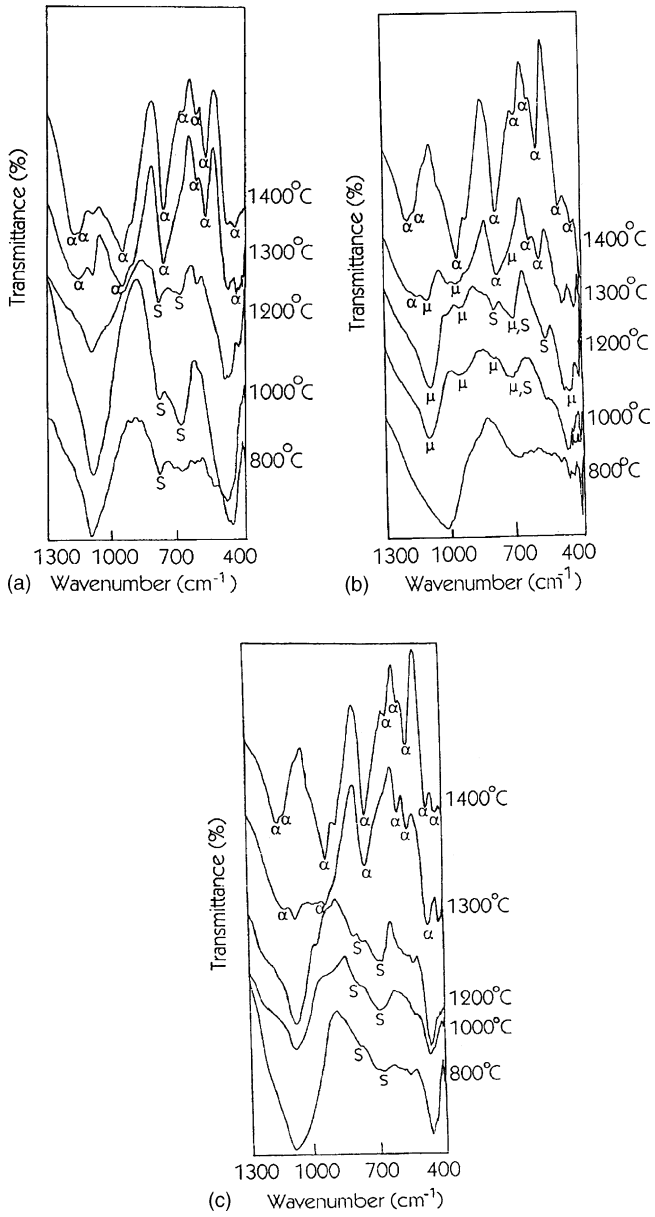

Fig. 4. (a) FTIR spectra of the powder sample CI obtained from rice husk ash calcined at different temperatures (800–1400 °C); S: $MgAl_2O_4$ spinel; α: α-cordierite; (b) FTIR spectra of the powder sample CII obtained from TEOS silica calcined at different temperatures (800–1400 °C); μ: μ-cordierite; S: $MgAl_2O_4$ spinel; α: α-cordierite; (c) FTIR spectra of the powder sample CIII obtained from fumed silica calcined at different temperatures (800–1400 °C); S: $MgAl_2O_4$ spinel; α: α-cordierite.

intensities of $[AlO_6]$ octahedra was maximum for CI obtained from rice husk ash and it was decreasing for CII obtained from TEOS and CIII obtained from fumed silica, with a predominant intensity of four-coordinated AlO_4, Al(IV) in CII. The maximum abundance of $[AlO_6]$ octahedral unit in CI (obtained from rice husk ash) preferred to interact with $[MgO_6]$ octahedral unit[27] rather than $[SiO_4]$ tetrahedral unit leading to initiation of crystallisation of $MgAl_2O_4$ spinel as observed from XRD results in Section 3.2.

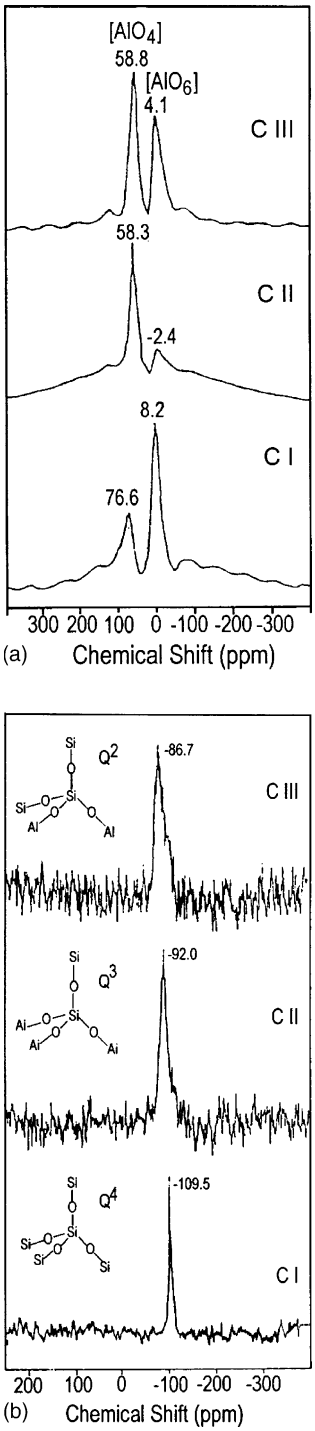

Fig. 5. (a) ^{27}Al MAS NMR spectra of the samples CI, CII and CIII obtained from different sources of silica calcined at 800 °C/1 h each. (b) ^{29}Si MAS NMR spectra of the samples CI, CII and CIII obtained from different sources of silica calcined at 800 °C/1 h each.

Fig. 5b shows ^{29}Si MAS NMR spectra of CI, CII and CIII calcined at 800 °C/1 h dwell each with the appearance of peak positions at −109.5, −92 and −86.7 ppm, respectively. The peak position at −109.5 ppm for CI was due to Q^4 state[28–30] for SiO_4 tetrahedra with Si (0Al) or Si

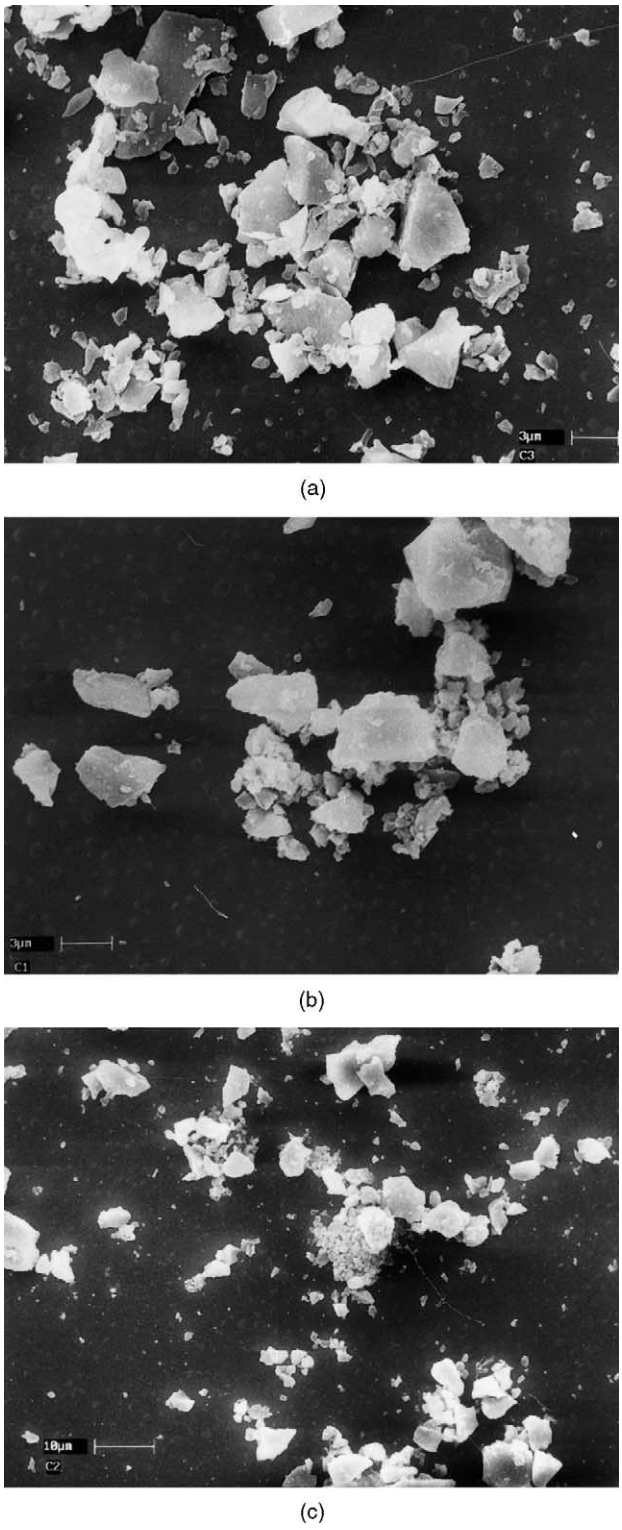

Fig. 6. (a) SEM photomicrograph of cordierite powders obtained from rice husk ash (CI), calcined at 1400 °C/1 h. (b) SEM photomicrograph of cordierite powders obtained from TEOS (CII), calcined at 1400 °C/1 h. (c) SEM photomicrograph of cordierite powders obtained from fumed silica (CIII), calcined at 1400 °C/1 h.

(4Si) forming $[Si(OSi)_4]$.[30] The peak position at around −109 ppm was due to the formation of cristobalite[28] and it was also confirmed by XRD results in Section 3.2. The peak position at −92 ppm for CII represented Q^3 state[28–30] for $[SiO_4]$ tetrahedra with Si (3Al) forming a ring structure of $[Si(OAl)_3(OSi)]$.[31,32] In this structure each Si atom was positioned with the next nearest neighbours of three Al atoms. For the sample CIII, the peak position at −86.7 ppm was due to Q^2 state[28–30] for SiO_4 tetrahedra with Si (2Al) forming a chain structure of $[Si(OAl)_2(OSi)_2]$.[31,32] In this structure each Si atom was positioned with the next nearest neighbours of two Al atoms. From the above observation it is to be noted that as there was poor intensity of $[AlO_4]$ tetrahedra (observed from ^{27}Al MAS NMR) in CI, instead of Al, the four Si atoms are next nearest neighbour of Si.

3.5. Scanning electron microscopy (SEM)

The SEM photographs of cordierite powders obtained from rice husk ash, TEOS and fumed silica, calcined at 1400 °C each are shown in Fig. 6a–c, respectively. The particles were irregular in shape and agglomerated in character in all the samples; there appeared no distinguishable morphology for three different sources of silica.

3.6. Particle size distribution

A comparatively wide size distribution, i.e. 105–290 nm with a average particle size of 180 nm was found for the sample CI obtained from rice husk ash silica (Fig. 7a) while for the sample CII obtained from TEOS, the mean particle size was 530 nm with a narrow size distribution from 490 to 580 nm (Fig. 7b) and the corresponding mean size of 145 nm with a size distribution from 90 to 205 nm was observed for the sample CIII obtained from fumed silica (Fig. 7c).

3.7. Conversion of gel to oxide powders—a tentative reaction steps

For the conversion of gel to oxide powders from three different sources of silica, i.e. rice hush ash, TEOS and fumed silica, DTA and XRD results confirmed the intermediate crystallisation of different phases at different temperatures towards the formation of α-cordierite (discussed in Sections 3.1 and 3.2). FTIR study (as discussed in Section 3.3) confirmed the characteristic bands of Si–O–Si symmetric and asymmetric stretching vibration in SiO_4 tetrahedra, Al–O bonds in AlO_6 octahedra and AlO_4 tetrahedra in the final product of α-cordierite. It could be proposed that during the transformation of gel to oxide powders, the cordierite was formed through different interactions of SiO_4 tetrahedra, AlO_4 tetrahedra, AlO_6 octahedra and MgO_6 octahedra. It was supported by ^{27}Al and ^{29}Si solid state NMR study of different materials i.e. CI, CII and CIII calcined at 800 °C (discussed in Section 3.4). From the results of DTA, XRD, FTIR and NMR studies, a tentative reaction pathway was established towards the formation of α-cordierite.

In case of CI obtained from rice husk ash, silica crystallised as cristobalite at 300 °C. The $MgAl_2O_4$ spinel was formed at about 1040 °C with the interaction of $[AlO_6]$

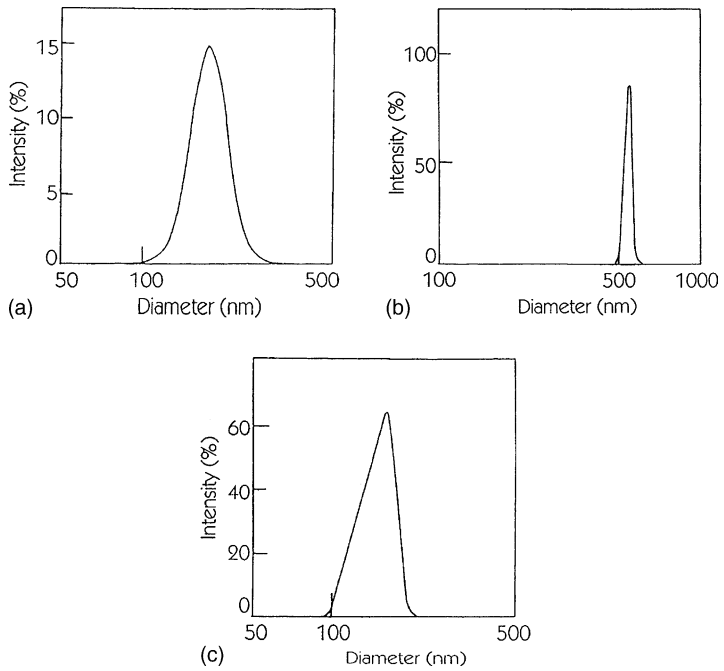

Fig. 7. (a) Particle size distribution of the powder sample CI obtained from rice husk ash, calcined at 1400 °C/1 h. (b) Particle size distribution of the powder sample CII obtained from TEOS, calcined at 1400 °C/1 h. (c) Particle size distribution of the powder sample CIII obtained from fumed silica, calcined at 1400 °C/1 h.

and $[MgO_6]$ octahedra following the transformation of α-cordierite at 1365 °C with the interaction of cristobalite and $MgAl_2O_4$ spinel.

(i) $[SiO_4] \rightarrow$ Cristobalite (at 300 °C);
(ii) $[AlO_6] + [MgO_6] \rightarrow MgAl_2O_4$ spinel (at 1040 °C); and
(iii) $Si(OAl)_2(OSi)_2 + MgAl_2O_4$ spinel $\rightarrow$ α-cordierite (at 1365 °C).

For the sample CII obtained from TEOS at 800 °C, $[SiO_4]$ tetrahedral unit interacted with $[AlO_4]$ tetrahedral forming $[Si(OAl)_3OSi]$ species followed by its reaction with $[MgO_6]$ octahedral at about 960 °C resulting the formation of μ-cordierite. At this temperature (960 °C), $[AlO_6]$ octahedral underwent the reaction with the remaining $[MgO_6]$ octahedral forming $MgAl_2O_4$ spinel. The transformation of α-cordierite was formed at about 1320 °C with the interaction of μ-cordierite and $MgAl_2O_4$ spinel.

(iv) $[SiO_4] + [AlO_4] \rightarrow Si(OAl)_3(OSi)$ (at 800 °C);
(v) $[Si(OAl)_3(OSi)] + [MgO_6] \rightarrow$ μ-cordierite (at 960 °C);
(vi) $[AlO_6] + [MgO_6] \rightarrow MgAl_2O_4$ spinel (at 960 °C); and
(vii) μ-cordierite $+ MgAl_2O_4$ spinel $\rightarrow$ α-cordierite (at 1320 °C).

For the sample CIII obtained from fumed silica, $[SiO_4]$ tetrahedra reacted with $[AlO_4]$ tetrahedra at 800 °C forming $[Si(OAl)_2(OSi)_2]$ species. However, $[AlO_6]$ octahedral species took part a complete reaction with $[MgO_6]$ octahedra at about 1010 °C to generate $MgAl_2O_4$ spinel. The α-cordierite was formed at about 1360 °C with the interaction of $Si(OAl)_2(OSi)_2$ and $MgAl_2O_4$ spinel.

(viii) $[SiO_4] + [AlO_4] \rightarrow Si(OAl)_2(OSi)_2$ (at 800 °C);
(ix) $[AlO_6] + [MgO_6] \rightarrow MgAl_2O_4$ spinel (at 1010 °C); and
(x) $Si(OAl)_2(OSi)_2 + MgAl_2O_4$ spinel $\rightarrow$ α-cordierite (at 1360 °C).

4. Conclusion

1. Cordierite ($Mg_2Al_4Si_5O_{18}$) powders were synthesised by using three different sources of silica: (i) utilising agro-based 'waste' material-rice husk ash; (ii) TEOS; and (iii) fumed silica and with other water-based precursor materials following sol–gel technique.
2. Crystallisation of α-cordierite from rice husk ash silica source occurred through the intermediate phases of cristobalite and $MgAl_2O_4$ spinel while that took place via the intermediate phases of μ-cordierite and $MgAl_2O_4$ spinel for TEOS source and $MgAl_2O_4$ spinel for fumed silica source. The above results were supported by DTA, XRD and FTIR studies.
3. The FTIR study also confirmed the characteristic bands of Si–O–Si symmetric and asymmetric stretching vibration in SiO_4 tetrahedra, Al–O bonds in AlO_6 octahedra and AlO_4 tetrahedra for the powders obtained from different sources of silica at different calcination temperatures.
4. The structural environment of Al and Si for the powders obtained from different sources of silica was confirmed by ^{27}Al and ^{29}Si solid state MAS NMR spectroscopy.
5. An irregular and agglomerated morphology of the particles were observed by SEM for all the samples, and a wide size distribution of the particles was found for the samples obtained from rice husk ash silica source.
6. A tentative reaction steps in conversion of gel to oxide powders obtained from three different sources of silica was established with the supporting evidences of DTA, XRD, FTIR, and ^{27}Al and ^{29}Si solid state MAS NMR studies.

Acknowledgements

The authors thank Dr. H.S. Maiti, Director of the Institute, for his kind permission to publish this paper. They are thankful to Mr. Gautam Gupta of Indian Institute of Technology, Kanpur for his contribution in helping the material preparation. Thanks are also due to the members of the Technical Ceramics, Membranes, SEM, and X-ray Sections of the Institute for helping in characterisation of the powders. The service rendered by Sophisticated Instruments Facility of Indian Institute of Science, Bangalore for recording ^{27}Al and ^{29}Si solid state MAS NMR spectra is thankfully acknowledged.

References

1. Ganguli, D. and Chatterjee, M., *Ceramic Powder Preparation: A Handbook*. Kluwer Academic Publishers, Boston, 1997, pp. 150–152.
2. Tsuchiya, T. and Ando, K., *J. Non. Cryst. Solids* 1990, **121**, 250.
3. Suzuki, H., Ota, K. and Saito, H., *Yogyo-Kyokai-Shi (J. Ceram. Soc. Jpn.)* 1987, **95**, 163.
4. Pal, D., Chakraborty, A. K., Sen, S. and Sen, S. K., *J. Mater. Sci.* 1996, **31**, 3995.
5. Nogami, M., Ogawa, S. and Nagasaka, K., *J. Mater. Sci.* 1989, **24**, 4339.
6. Evans, D. L., Fischer, G. R., Geiger, J. E. and Martin, F. W., *J. Am. Ceram. Soc.* 1980, **63**, 629.
7. Petrovic, R., Janackovic, D., Zec, S., Drmanic, S. and Kostic-Gvozdenovic, L., *J. Mater. Res.* 2001, **16**, 451.
8. Douy, A., Organic gels in the preparation of silicate powders: example of mullite and cordierite. In *Chemical Processing of Advanced Materials*, ed. L. L. Hench and J. K. West. Wiley, New York, 1992, pp. 585–594.
9. Gopi Chandran, R. and Patil, K. C., *Br. Ceram. Trans.* 1993, **92**, 239.
10. Chandrasekhar, S., Satyanarayana, K. G., Pramada, P. N., Raghavan, P. and Gupta, T. N., *J. Mater. Sci.* 2003, **38**, 3159.
11. Indian Patent Application No. 1267/DEL/01.
12. Indian Patent Application No. 1269/DEL/01.
13. Brinker, C. J. and Scherer, G. W., *Sol–Gel Science: The Physics and Chemistry of Sol–Gel Processing*. Academic Press, USA, 1990, p. 108.
14. Chen, Y. F. and Vilminot, S., *J. Sol-Gel Sci. Tech.* 1995, **5**, 41.
15. Takayuki, B., Shigeo, H., Yasumori, A. and Okada, K., *J. Eur. Ceram. Soc.* 1996, **16**, 127.

16. Naskar, M. K., Chatterjee, M. and Lakshmi, N. S., *J. Mater. Sci.* 2002, **37**, 343.
17. Selvaraj, U., Komarneni, S. and Roy, R., *J. Am. Ceram. Soc.* 1990, **73**, 3663.
18. Meyer, M., Hempelmann, R., Mathur, S. and Veith, M., *J. Mater. Chem.* 1999, **9**, 1755.
19. Lin, C.-P. and Wen, S.-B., *J. Am. Ceram. Soc.* 2002, **85**, 1477.
20. Schroeder, R. A. and Lyons, L. L., *J. Inorg. Nucl. Chem.* 1966, **28**, 1155.
21. Serna, C. J., Rendon, J. L. and Iglesias, J. E., *Spectrochim. Acta. Part A* 1982, **38A**, 797.
22. Nyquist, R. A. and Kagel, R. O., *Infrared Spectra of Inorganic Compounds*. Academic Press, New York, 1971, pp. 37, 116, 188.
23. Blackell, C. S. and Patton, R. L., *J. Phys. Chem.* 1984, **88**, 6135.
24. Wu, Y., Chmelka, B. F., Pines, A., Davis, M. E., Grobet, P. J. and Jacobes, P. A., *Nature* 1990, **346**, 550.
25. Turner, G. L., Kirkpatrick, R. J., Risbud, S. H. and Oldfield, E., *Am. Ceram. Soc. Bull.* 1987, **66**, 656.
26. Komarneni, S. and Roy, R., *J. Am. Ceram. Soc.* 1986, **69**, C-42.
27. Livage, J., Babonneau, F., Chatry, M. and Coury, L., *Ceram. Int.*, 1997, 23.
28. Smith, J. V. and Blackwell, C. S., *Nature* 1983, **303**, 223.
29. Selvary, U., Rao, K. J., Rao, C. N. R., Klinowski, J. and Thomas, J. M., *Chem. Phys. Lett.* 1985, **114**, 24.
30. Laridjani, M., Lafontaine, E., Bayle, J. P. and Judeinstein, P., *J. Mater. Sci.* 1999, **34**, 5945.
31. Fyfe, C. A., Gobbi, G. C., Klinowski, J., Putnis, A. and Thomas, J. M., *J. Chem. Soc. Commun.*, 1983, 556.
32. Fyfe, C. A., Gobbi, G. C. and Putnis, A., *J. Am. Chem. Soc.* 1986, **108**, 3218.